# Changes to simulated global atmospheric composition resulting from recent revisions to isoprene oxidation chemistry

M. Anwar H. Khan[a], Billie-Louise Schlich[a], Michael E. Jenkin[b], Michael C. Cooke[a,1], Richard G. Derwent[c], Jessica L. Neu[d], Carl J. Percival[d], Dudley E. Shallcross[a,e]*

[a]Biogeochemistry Research Centre, School of Chemistry, University of Bristol, Cantock's Close, Bristol BS8 1TS, UK

[b]Atmospheric Chemistry Services, Okehampton, Devon, EX20 4QB, UK

[c]rdscientific, Newbury, Berkshire, UK

[d]NASA Jet Propulsion Laboratory, California Institute of Technology, 4800 Oak Grove Dr, Pasadena, CA 91109, USA

[e]Department of Chemistry, University of the Western Cape, Robert Sobukwe Road, Bellville, 7375, South Africa.

[1]Currently at Met Office, Exeter, UK

*Author to whom correspondence should be sent

E-mail: d.e.shallcross@bristol.ac.uk

Phone: +44 (0) 117 928 7796

**Abstract**

Recent revisions to our understanding of the oxidation chemistry of isoprene have been incorporated into a well-established global atmospheric chemistry and transport model, STOCHEM-CRI. These revisions have previously been shown to increase the production and recycling of $HO_x$ radicals at lower $NO_x$ levels characteristic of the remote troposphere. The main aim of this study is to assess the resultant broader changes to atmospheric composition due to the recent revisions to isoprene oxidation chemistry. The impact of the increased isoprene-related $HO_x$ recycling is found to be significant on the reduction of volatile organic compounds (VOCs) lifetime, e.g. a decrease in isoprene's tropospheric burden by ~17%. The analysis of lifetime reduction of the potent greenhouse gas, methane, associated with the increased $HO_x$ recycling, suggests its significant lifetime reduction by ~5% in terms of the current literature. The revisions to the isoprene chemistry also reduce the amount of ozone (by up to 10%), but provide a significant increase in $NO_3$ (by up to 30%) over equatorial forested regions, which can alter the oxidizing capacity of the troposphere. The calculated mixing ratios of formic acid are decreased which in turn leads to an increase in the inferred concentrations of Criegee intermediates due to reduced loss through reaction with formic acid (up to 80%) over the dominant isoprene emitting regions.

**Keywords:** Isoprene chemistry; $HO_x$ recycling; oxidation cycle; atmospheric lifetime; equatorial region.

## 1. Introduction

Isoprene (2-methyl-buta-1,3-diene) is emitted into the atmosphere on a similar scale to methane, averaging approximately 600 Tg $year^{-1}$ and thus positioning the species as the most abundant non-methane hydrocarbon emitted into the troposphere (Guenther et al., 2012; Sindelarova et al., 2014). Approximately 85-90% of all isoprene emissions are from biogenic sources (Guenther et al., 2012), with the remainder emitted from anthropogenic sources (e.g. vehicular exhaust) (Borbon et al., 2001; Reimann et al., 2000; Khan et al., 2018) and oceanic sources (Arnold et al., 2009). Isoprene emission from plants is directly linked to photosynthesis, as the formation of the $C_5$ compound is non-trivial requiring a significant amount of energy (Delwiche et al., 1993; Sharkey and Yeh, 2001). Therefore, the highest mixing ratios of isoprene are seen across the tropics over landmasses where most of the Earth's biomass is located. Areas of elevated isoprene mixing ratios can also be seen over Russia and Canada in a biome known as the boreal forest. Regions of boreal forest or Taiga are characterised by coniferous trees situated in a highly seasonal climate, with cold seasons seeing extreme low temperatures and snow coverage. In spring, the melted snow reveals vast forests that can achieve high rates of photosynthesis and hence realise a significant source of isoprene for the global budget (Fuentes et al., 1999).

Isoprene is not thought to be a major threat to human health in its unreacted form, but it is highly reactive with a relatively short atmospheric lifetime (e.g. 2.8 hours with respect to reaction with $10^6$ molecule $cm^{-3}$ OH at 298 K; Atkinson and Arey, 2003) and possesses a greater risk when its subsequent atmospheric reaction products are considered. For example, its complex atmospheric reactions have significant impact on the distribution and variability of the key short-lived climate forcers: tropospheric ozone, secondary organic aerosol (SOA) and methane (Fiore et al., 2012). In low $NO_x$ environments e.g. the Amazon, isoprene derived SOA is formed through the oxidation of isoprene (Lin et al., 2012), whereas in high $NO_x$ environments such as cities, the oxidation of isoprene can potentially enhance local or regional scale production of ozone (Geng et al., 2011). Incidence of these species in populated regions increases the prevalence of respiratory diseases and damages the environment and infrastructure.

High levels of OH are maintained from initial oxidation of volatile organic compounds (VOCs), which forms chain-propagating species and regenerates the oxidant, OH. Isoprene oxidation products have been reported to be responsible for the formation of cloud condensation nuclei (CCN) leading to a cooling effect (Zhu et al., 2017). However, a recent study showed that isoprene produced a modest amount of aerosol that are oxidized in mixtures of atmospheric vapours suppressing both particle number and mass of SOA (McFiggans et al., 2019). The competitive reaction of isoprene with OH also has an increasing influence on the lifetime of methane and other trace gases, and a resultant impact on global warming.

Atmospheric observations in areas characterised by low $NO_x$ concentrations (e.g. the Amazon and Borneo) have shown levels of OH radicals to be much higher than those simulated using traditional understanding of isoprene oxidation (Lelieveld et al., 2008; Pugh et al., 2010; Müller et al., 2019). This highlighted an incomplete representation of recycling mechanisms for $HO_x$ radicals (i.e. OH and $HO_2$) that could operate at low $NO_x$ levels. More recent studies of isoprene oxidation have led to substantial improvements in understanding, as a result of theoretical studies (Peeters et al., 2009; 2014) and laboratory investigations (Wennberg et al., 2018). Updated isoprene mechanisms incorporating this understanding show increased production and recycling of $HO_x$ radicals at lower $NO_x$ levels (Wennberg et al., 2018; Archibald et al., 2010; Jenkin et al., 2019). This illustrates that accurate representation of atmospheric isoprene oxidation chemistry is an essential component of models aiming to assess the impact of isoprene emissions on air quality, human health and climate change.

The reduced representation of isoprene degradation in the Common Representative Intermediates (CRI) mechanism has been recently updated, and implemented into the chemical transport model, STOCHEM-CRI (Jenkin et al., 2019). That study illustrated that the updates resulted in increased concentrations of $HO_x$ radicals in regions characterised by low $NO_x$ and high isoprene emissions. In this study, we report the broader impacts of the mechanistic updates (including the effects of increased $HO_x$ recycling) on the global-scale composition of the troposphere, using STOCHEM-CRI.

## 2. Model description

STOCHEM is a 3-dimensional model that utilises a 3h time step for the advection of its 50,000 constant mass air parcels that represent the Earth's troposphere (Collins et al., 1997). It is within these isolated air parcels that the chemical reactions and photochemical dissociations leading to the loss and production of trace gases are considered to be taking place. A Lagrangian approach is employed with regards to the transport processes. The main advantage of a Lagrangian approach is that the chemistry and transport processes can be uncoupled allowing the local determination of a chemistry timestep. The chemistry scheme uses a backwards Euler solver using a timestep of 5 minutes allowing an accurate solution of chemical ordinary differential equations to be evaluated. The meteorological data concerning pressure, temperatures, winds, clouds, humidity, tropopause heights, precipitation, boundary layer depth and surface parameters are taken from the UK Met Office Unified Model (UM) for the year 1998 which are at a resolution of 1.25° longitude, 0.8333° latitude and 12 unevenly spaced vertical levels with 1 km level thickness near the surface.

Advection of the 50000 constant mass Lagrangian air parcels is described by wind fields generated from the UK Met Office Unified Model (UM) for the year 1998 (Cullen, 1993). The archived meteorological data used contains 6 hourly wind fields for horizontal and vertical winds, with an advection time-step set to 3 hours. This allows the wind fields to be linearly interpolated with respect to time, using a cubic polynomial in the vertical domain

and a bi-linear method in the horizontal. Additionally, a fourth-order Runge-Kutta advection scheme is used to calculate the new Lagrangian cell positions, and an analogous interpolation method is used for the pressure, temperature and humidity of the cells.

A hybrid-pressure vertical coordinate is used in the STOCHEM model, the main advantage of using a hybrid system being that the 'terrain-following' nature of the coordinate avoids the issue of intersecting ground topography. The two methods used for treatment of the boundary layer in STOCHEM draw parallels from those reported in the NAME model by Ryall et al. (1998). These methods allow the boundary layer, the region between the Earth's surface and the free troposphere, to be estimated from the temperature and wind fields provided by the archived meteorological data. The STOCHEM model uses a parameterisation where, when an air parcel is established in the boundary layer, the vertical coordinate is subsequently randomly reassigned within the boundary layer plus a small calculated extra thickness to allow transport out of the layer (Ehhalt et al., 1992).

The inter-mixing of parcels in regions of convective clouds can significantly vary species concentrations within and above the boundary layer. The model's archived meteorological data provides information concerning the convective cloud cover, convective cloud top height, convective cloud bottom height and convective precipitation, with these fields used to parameterise convective mixing due to it being a sub-grid scale process (Collins et al., 1999)

The chemical mechanism used previously in STOCHEM was the Common Representative Intermediates mechanism version 2, reduction 5 (CRI v2-R5). Developed initially by Jenkin et al. (2008) with subsequent additions by Watson et al. (2008) reduction 5 of the mechanism was the most reduced variant, making it suitable for global modelling due to its traceability to the prevailing version of the Master Chemical Mechanism at the time (MCM v3.1). For the present study, the mechanism was updated to CRI v2.2. As described by Jenkin et al. (2019), CRI v2.2 contains a series of updates to the chemistry of isoprene degradation, and performs consistently with the current version of the Master Chemical Mechanism, MCM v3.3.1 (http://mcm.york.ac.uk). The complete isoprene oxidation scheme contains 186 reactions of 56 closed shell and free radical species, and is an order of magnitude smaller than MCM v 3.3.1. The details of the oxidation scheme can be found in Jenkin et al. (2019) including a full description of those features that result in increased $HO_x$ recycling at low $NO_x$ levels. Addition of the Criegee field involved the inclusion of 17 individual stabilized Criegee intermediates (sCIs) along with explicit formation from ozonolysis reactions of the alkenes and loss processes by unimolecular decomposition, and/or reaction with water, water dimer, sulphur dioxide and formic acid (see Supplementary Information Table S1). The complete Criegee field scheme contains 17 new species, which compete in 58 additional reactions. More details of the Criegee species and their formation and loss reactions can be found in Caravan et al. (2020) and Chhantyal-Pun et al. (2019).

The emission profile for STOCHEM consists of three different categories: surface emissions, stratospheric sources and 3-dimensional emissions. Emissions that fall under

surface emissions are biomass burning, vegetation, ocean and soil and are dispersed using monthly two-dimensional source maps at a resolution of 5° longitude by 5° latitude (Olivier et al., 1996). The STOCHEM emissions inventory is discussed in detail in Khan et al. (2014). In STOCHEM, a simple approach of emitting isoprene is used at a rate proportional to the cosine of the solar zenith angle during the day with no emissions at night. This is because, unlike other biogenic hydrocarbons such as monoterpenes, isoprene has a direct relationship with the photosynthetic activity of plants (Seinfeld and Pandis, 2006). The rate is adjusted to give the appropriate total emission over a month for each grid square. These monthly emissions were taken from Guenther et al. (1995) and include the appropriate scaling of isoprene emissions with temperature. In the STOCHEM model, surface emissions are added on a 5 degree latitude by 5 degree longitude Eulerian grid square basis. This is too coarse (600 km × 400 km at mid-latitudes) to resolve individual centres of pollution but it is large enough to give an average Lagrangian cell occupancy of approximately two Lagrangian cells within the boundary layer per grid square in the mid-latitudes. After each 3-hour advection time-step, the surface emissions are distributed equally over all the cells within the boundary layer for a particular emission grid square. If there are no cells within the boundary layer for a particular emissions grid square then those emissions are stored during the next advection time-step or until a cell does pass through the emissions grid square. While the advection time-step is set at 3-hours, the storage contains only 1/2920 of the annual emissions and so impacts on the chemistry of the stored emission are small. Finally, all emissions are converted into units of molecules per second per grid square.

The prevalent removal processes for chemical species within air parcels at the boundary layer are dry deposition and wet deposition. Dry deposition rates depend on whether a Lagrangian air parcel is treated as above land or ocean. The removal of soluble species through dissolution in precipitation in known as wet deposition. These dissolved components can originate in the environment during nucleation or incorporate into precipitation as it falls. Equations used for wet deposition in STOCHEM combine species dependent scavenging coefficients with scavenging profiles and precipitation rates to calculate wet deposition loss rates. More details about the dry and wet deposition implemented in STOCHEM can be found in Percival et al. (2013).

Two simulations were conducted to investigate the impacts of the updated isoprene oxidation mechanism on global scale atmospheric composition and oxidizing capacity. The base case simulation was based on the reference conditions described in Utembe et al. (2010) using CRI v2, with the addition of Criegee field as in Caravan et al. (2020). The Criegee field described in the Supplementary Information allowed enhanced modelling of the atmospheric fate of formic acid. Another simulation referred to as ‘ISOP’ was based on the updated version of the model with inclusion of the CRI v2.2 isoprene chemistry described in Jenkin et al. (2019) along with the Criegee field. A streamlined overview has been given in Scheme 1 to focus the most significant changes in ISOP from base case. All simulations were run with

meteorology from 1998 for a period of five years and the results were taken from the fifth year.

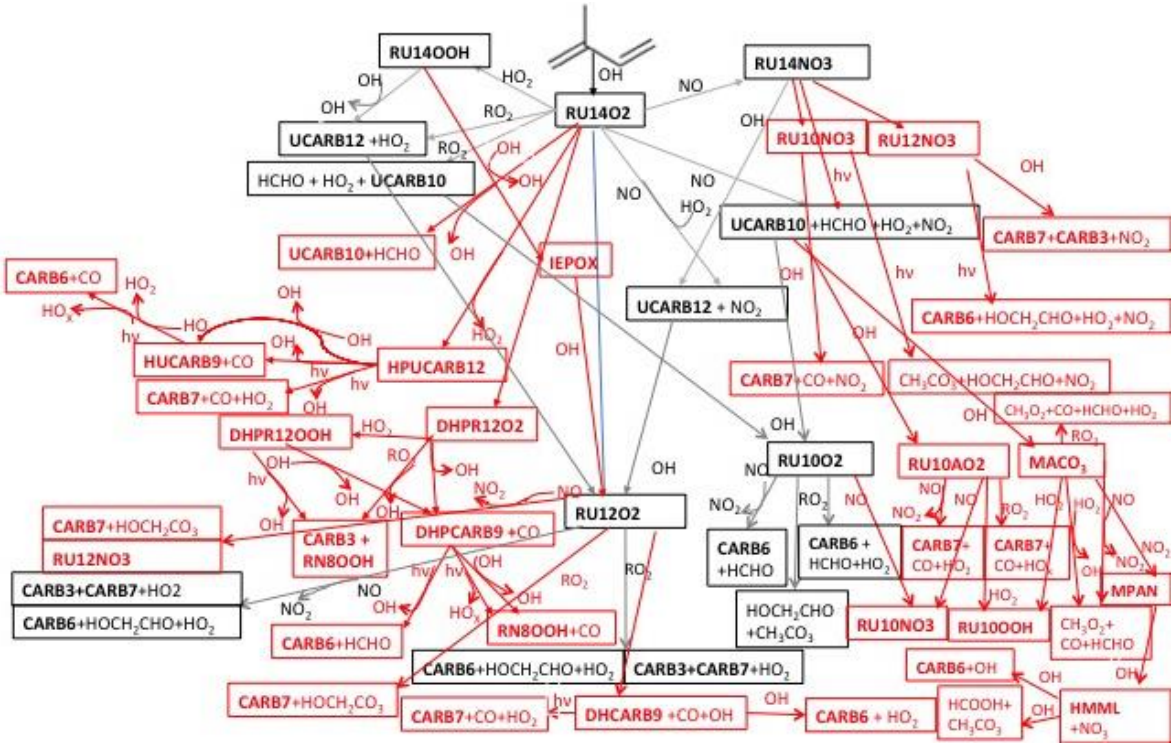


**Scheme 1:** Schematic to show an overview of the important reactions added to STOCHEM-CRI for the revision of isoprene oxidation chemistry. New reactions are shown in red. More detail about the oxidation scheme can be found in Jenkin et al. (2019)

### 3. Results and Discussion

The results of the ISOP simulation showed increased $HO_x$ production, resulting from the updates to the isoprene degradation chemistry in CRI v2.2. This led to an increase in the OH and $HO_2$ tropospheric burdens of 6.4% and 0.8%, respectively (Table 1). Methane ($CH_4$) is a potent greenhouse gas, and its reaction with OH is the second most important sink for OH in the troposphere. The loss flux of $CH_4$ + OH in ISOP was increased by 40 Tg/y (6% from base case) resulting in a decrease in the atmospheric $CH_4$ lifetime of 6.8 years by 0.5 years (7.3% from base case). Thus, the lifetime reduction of $CH_4$ by 0.5 years in the study (~5% from literature value) could be significant in terms of reducing warming of the Earth's atmosphere (Collins et al., 2018). The tropospheric lifetime of $CH_4$ estimated is on the low side of the studies (e.g. Sonnemann and Grygalashvyly, 2014; Stevenson et al., 2006; Prinn et al., 2005; Prather et al., 2012) with a range of 7 to 10 years. The OH field in the model is in good agreement with other studies (Cooke, 2010), however the possible warm bias of the temperature field in our model can have increased rate of oxidation which is likely to be the reason for the shorter lifetime of $CH_4$.

The increase in the OH concentration results in a shortened lifetime of all VOCs, including very reactive, short-lived biogenic VOCs e.g. isoprene, α-pinene, β-pinene. This, in turn, leads to a decrease in their tropospheric burdens of 17%, 4% and 8%, respectively. The

simulated OH concentration during March in the base case ($3.7 \times 10^5$ molecule/cm$^3$) is found to be lower when it is compared with the observed OH concentration ($(5.3 \pm 4.6) \times 10^5$ molecule/cm$^3$) during March 2014 over Amazon (Liu et al., 2016). From the increased OH concentrations (20-50%) in the equatorial forested regions after incorporating the new isoprene degradation mechanism (Jenkin et al., 2019), the increased OH concentration in ISOP ($4.9 \times 10^5$ molecule/cm$^3$) reduces the disagreement between the model and the measurement significantly. The degree of isoprene $HO_x$ recycling is comparable with the study of Müller et al. (2019) who simulated the most recent mechanism for the oxidation of biogenic VOCs using the Model of Atmospheric composition at Global and Regional scales using Inversion Techniques for Trace gas Emissions (MAGRITTE v1.1) and found increased OH concentrations by up to 40% over western Amazonia in the boundary layer and 10-15% over the south-eastern US and Siberia.

**Table 1.** The annual mean global burden for the base and ISOP run and percentage difference for ISOP for a selection of species

| **Species** | **Base (Tg)** | **% change** |
|---|---|---|
| OH | $2.46 \times 10^{-4}$ | 6.4 |
| $HO_2$ | $2.6 \times 10^{-2}$ | 0.8 |
| $O_3$ | $3.16 \times 10^{2}$ | -1.5 |
| $NO_x$ | $4.98 \times 10^{-1}$ | -1.3 |
| $NO_3$ | $1.17 \times 10^{-2}$ | 1.0 |
| $HNO_3$ | $5.03 \times 10^{-1}$ | -0.2 |
| $CH_4$ | $4.39 \times 10^{3}$ | -1.5 |
| HCOOH | $1.47 \times 10^{-1}$ | -43.5 |
| Isoprene | $1.64 \times 10^{-1}$ | -16.7 |
| α-pinene | $1.37 \times 10^{-2}$ | -4.3 |
| β-pinene | $1.20 \times 10^{-2}$ | -8.0 |
| $RO_2$ | $4.78 \times 10^{-2}$ | -6.5 |
| $RONO_2$ | $9.11 \times 10^{-1}$ | 181.9 |
| PANs | 4.48 | -19.6 |

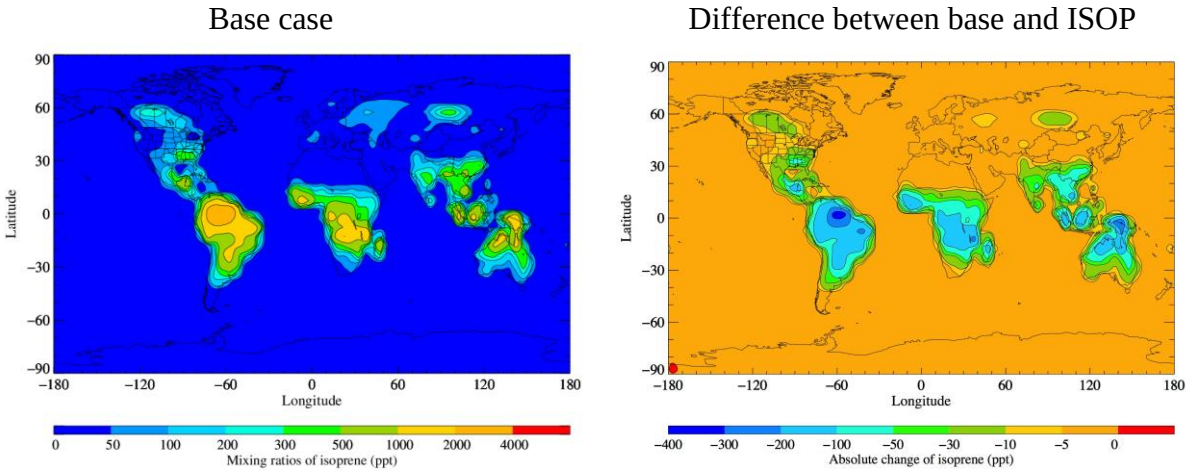


**Fig. 1.** a) The annual concentration of isoprene in the base case, b) The annual absolute change in isoprene concentration between the base run and ISOP, Note: absolute change= ISOP-base

Isoprene's short atmospheric lifetime results in its mixing ratios being localised to emission regions e.g. Amazon rainforest, southern Africa, parts of south East Asia and northern Australia (Figure 1a). The large emissions and short lifetime of isoprene has caused problems in global models because of the reduction of OH concentrations over isoprene source regions. However, the increase in modelled OH concentrations over equatorial forest regions in the ISOP simulation decreases the tropospheric isoprene burden by 17% and shortens the tropospheric lifetime from 2.7 days to 2.2 days. As a result, the isoprene mixing ratios are reduced by up to 300 ppt in the equatorial forested regions (Figure 1b). We compared our modelled isoprene mixing ratio data with some measurement data from around the tropical region (Table 2) and found a disagreement between model and measurement for most of the tropical stations. The increased isoprene-related $HO_x$ recycling in the ISOP simulation decreases the isoprene mixing ratios (see Figure 1b) in the Amazon basin, Venezuela, Surinam, Borneo and Peru, which slightly improves the model-measurement disagreement in Amazon, Venezuela and Borneo (see Table 2). However, the disagreement is still significant which is most likely due to the overestimation of isoprene emissions over the Tropics. In our model run, we used the MEGAN emission inventory, which has a factor of 2 uncertainty due to errors in land cover and meteorological driving variables (Guenther et al., 2012). The satellite top-down estimates (Barkley et al., 2013; Marais et al., 2014; Bauwens et al., 2016) suggested that the emission inventories (e.g. MEGAN, POET) used in the global model overestimated isoprene emissions over the Tropics. Comparing with the surface isoprene flux observations over Africa, Marais et al. (2014) found overestimated isoprene emissions from the MEGAN emission inventory but good agreement with the satellite top-down estimate. A recent box modeling study by Mouchel-Vallon et al. (2020) also reported that the box model with more detailed isoprene chemistry (reactions from Master Chemical Mechanism, MCM 3.3.1 and Generator for Explicit Chemistry and Kinetics of Organics in the Atmosphere, GECKO-A) and the MEGAN emission inventory overestimated the surface

isoprene mixing ratios over the Amazon by a factor of 7. To investigate the uncertainty of the MEGAN emission inventory, a sensitivity study was conducted with reducing MEGAN isoprene emissions to the Base case by a factor of 2 in the runs referred to as 'Base-RE'. The results from Base-RE simulation showed a significant improvement of the model-measurement disagreement of isoprene mixing ratios over tropical forest area (see Table 2) suggesting that the overestimated isoprene mixing ratios in Base case is most likely caused by the MEGAN emission inventory.

In addition, the resolution ($5^o \times 5^o$) used for emissions, inter-parcel exchange and mapping is coarse which is roughly the size of a small country, which makes it difficult to compare modelled data with measurements taken in areas of low or high emissions. Also, the model was run with 1998 meteorology whereas the measurements were from a variety of years, meaning there is likely to be some variation between measured and modelled data.

**Table 2.** Comparison of measured daytime isoprene mixing ratios (ppb) with model daytime isoprene mixing ratios (ppb) for base and ISOP cases. Note: The model values are adjusted for daytime (from 6 am to 6 pm) using 24 hour averaged model output data.

| Location | Time | Measured | Base | ISOP | Base-RE |
|---|---|---|---|---|---|
| Amazon Basin[1] (2S, 60W) | Jul | 2.2 (1.2-3.2) | 6.10 | 5.53 | 1.95 |
| Amazon Basin[2] (2S, 60W) | Annual | 2.4 (1.0-5.2) | 5.07 | 4.58 | 1.68 |
| Amazon Basin[3] (2S, 60W) | Jul-Aug | 2.0 (1.1-2.7) | 6.03 | 5.45 | 1.95 |
| Amazon Basin[4] (2-4S, 59-61W) | Sep | 2.2 (0.2-5.4) | 6.96 | 6.44 | 2.44 |
| *Peru[5] (~2 m) (5S, 77W) | Jul | 3.31 | 2.03 | 1.88 | 0.72 |
| *Peru[5] (91m-1.2 km) (5S, 77W) | Jul | 1.39 | 1.23 | 1.11 | 0.41 |
| Venezuela, Buja[6] (9N, 62W) | Sep | 3.3 | 2.48 | 2.11 | 0.87 |
| Venezuela, Auyantepuy[6] (6N, 62W) | Apr | 1.6 ± 1.1 | 2.10 | 1.79 | 0.62 |
| Venezuela, Calabozo[7] (9N, 67W) | Sep-Oct | 1.6 ± 0.7 | 3.37 | 3.05 | 1.10 |
| Venezuela, Calabozo[7] (9N, 67W) | Mar-Apr | 0.8 ± 0.2 | 0.97 | 0.81 | 0.31 |
| Venezuela, Parupa[7] (6N, 62W) | Jan-Feb | 0.5 ± 0.2 | 1.24 | 1.03 | 0.42 |
| Surinam[8] (2-7N, 54-58W) | Mar | 0.9 | 2.32 | 1.89 | 0.78 |
| Borneo, Malaysia[9] (4N, 117E) | April | 1.1 (0.28-2.8) | 1.99 | 1.58 | 0.66 |
| Borneo, Malaysia[10] (4N, 117E) | June-July | 1.06 (0.05-2.47) | 1.11 | 0.92 | 0.37 |

Note: *The reported values are median. References: [1]Rasmussen et al. (1988), [2]Greenberg et al. (1984), [3]Zimmerman et al. (1988), [4]Fu et al. (2019), [5]Helmig et al. (1998), [6]Donoso et al. (1996), [7]Holzinger et al. (2002), [8]Crutzen et al. (2000), [9]Emmerson et al. (2016), [10]Langford et al. (2010).

The *in-situ* measurements of isoprene are sparse and limited in tropical rainforest regions (Jones et al., 2011; Hewitt et al., 2010). Over the last decade, global satellite observations of formaldehyde (HCHO), a high-yield, prompt oxidation product of isoprene, have been used to provide additional top-down constraints on regional and global isoprene emissions and assess their seasonal and inter-annual variability (Millet et al., 2008; Stavrakou et al., 2009; Barkley et al., 2013; Marais et al., 2014; Bauwens et al., 2016). However, HCHO is also a product of other VOC reactions, and satellite HCHO columns have been shown to reflect only about a quarter of the reduction in isoprene emissions associated with severe drought in the Missouri Ozarks region of the US (Zheng et al., 2017). The lack of HCHO

column response has been attributed to a photochemical feedback whereby reduced isoprene emission increases the oxidation capacity available to generate HCHO from other VOC sources (Zheng et al., 2017). Furthermore, the link between HCHO and isoprene is a strong nonlinear function of $NO_x$, with the prompt yield increasing by a factor of 3 over a range of $NO_x$ values representing remote to urban conditions, and background HCHO increasing by a factor of 2 over this $NO_x$ range (Wolfe et al., 2016). Marais et al. (2012) suggested that the uncertainties in the chemical transport modelling of isoprene oxidation chemistry could be as large as 90% under relatively low-$NO_x$ conditions typical of the tropics, providing large errors when HCHO is used to infer isoprene emissions. Additionally, the increased isoprene-related $HO_x$ recycling in the study leads to a decrease in the lifetime of isoprene resulting in increase the ratio, [HCHO]/[isoprene] by up to 50% over the tropical forest region (see Supplementary Information Figure S1), the result is consistent with the findings of Bates and Jacob (2019). Thus, the indirect remote sensing approach could lead to large errors in isoprene emission estimates, depending on the background conditions, if one wished to quantify long term emissions of isoprene from satellite measurements of HCHO. The impact of increased $HO_x$ chemistry and the resultant error in retrieved isoprene emissions is a critical factor that needs to be considered. Alternatively, the direct satellite measurements of isoprene (Fu et al., 2019) could be the viable option for determining isoprene emissions over large ecosystems such as tropical rainforests for a full seasonal cycle over multiple years.

The global burden of simulated peroxy radicals ($RO_2$) is found to be reduced from the base to ISOP simulation by 6.5% (Table 1) which is mainly as a result of the significant reduction in the burdens of the dominant isoprene-derived peroxy radicals: RU14O2 (MCM v3.3.1 analogues: ISOPAO2, CISOPAO2, ISOPBO2, ISOPCO2, CISOPCO2, ISOPDO2, ISOP34O2; 0.4 Gg and 24%), RU12O2 (MCM v3.3.1 analogues: C57O2, C57AO2, C58O2, C58AO2, C59O2, HC4ACO3, HC4CCO3; 1.3 Gg and 66%) and RU10O2 (MCM v3.3.1 analogues: HMVKAO2, HMVKBO2, MACROHO2; 1.2 Gg and 69%). Such an observation arises mainly from the newly implemented peroxy radical isomerisation reactions for RU14O2, particularly at lower $NO_x$ levels. These reactions have the effect of both suppressing the concentration of RU14O2 itself and reducing its fractional conversion to RU12O2 and RU10O2 (e.g. via the RU14O2 + NO reaction) by providing additional competing loss routes that do not result in the production of peroxy radicals. The associated decrease in the collective flux through $RO_2$ + NO reactions has a reducing effect on ozone formation, which contributes to a resultant reduction in the burden of ozone by 1.5% from the base case (Table 1).

The formation of first generation isoprene nitrates by reaction of isoprene peroxy radicals (RU14O2) with NO was assumed to have a branching ratio of 10% in ISOP which is within the range of 4% to 15% suggested by previous laboratory and field studies (Chen et al., 1998; Chuong and Stevens, 2002; Sprengnether et al., 2002; Horowitz et al., 2007; Paulot et al., 2009; Lockwood et al., 2010; Nguyen et al., 2014; Xiong et al., 2015; Schwantes et al., 2015). In the updated chemistry, the further oxidation of RU14NO3 generates two new second-generation nitrates, RU12NO3 and RU10NO3 (Scheme 1) with details shown in Jenkin et al. (2019) with global burdens of 0.08 and 0.83 Tg, respectively, which lead to an

overall increase the global burden of organic nitrates by 0.91 Tg (~180% from base case). The spatial distributions of RU12NO3 and RU10NO3 are very similar to that of RU14NO3, but the mixing ratios of RU12NO3+RU10NO3 is found to be ~3 times higher than that of RU14NO3 (see Supplementary Information Figure S2). The comparison of model isoprene, ISOPOOH, IEPOX and organic nitrates with the SEAC$^4$RS measurements (compiled from Fisher et al., 2016 and Müller et al., 2019) showed improved agreement due to increased isoprene-related $HO_x$ recycling in the ISOP simulation. For organic nitrates, there is a large model overestimation throughout the troposphere (see Figure S3). The losses of organic nitrates through deposition (wet and dry), hydrolysis and heterogeneous uptake by aqueous aerosols were not considered in the model, which can be significant over vegetated areas (Romer et al., 2016; Fisher et al., 2016). This would likely lead to overestimation of model $RONO_2$ mixing ratios in the troposphere. Considering the loss rate of organic nitrates into the aerosol phase as $6 \times 10^{-6}$ $s^{-1}$, the same as $HNO_3$ (Derwent et al., 2003), we performed another simulation in a run hereafter referred to as ON-AER. The simulation results showed a significant improvement of the model-measurement disagreement of organic nitrates with the reduction of the overestimation by ~60-80% (Figure S3).

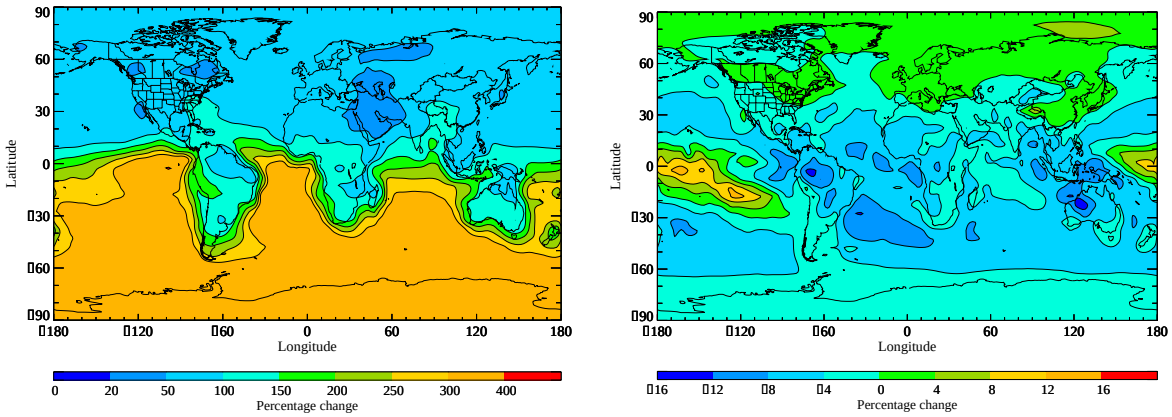


(a) (b)

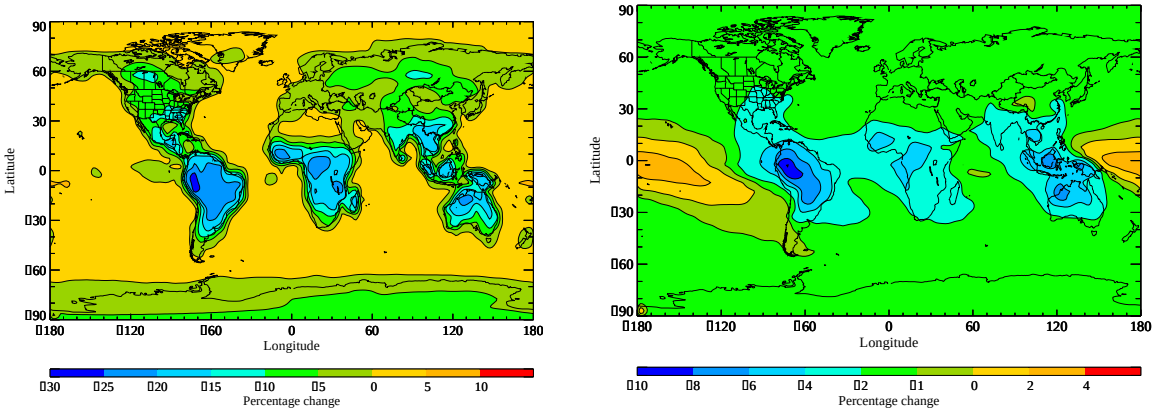


(c) (d)

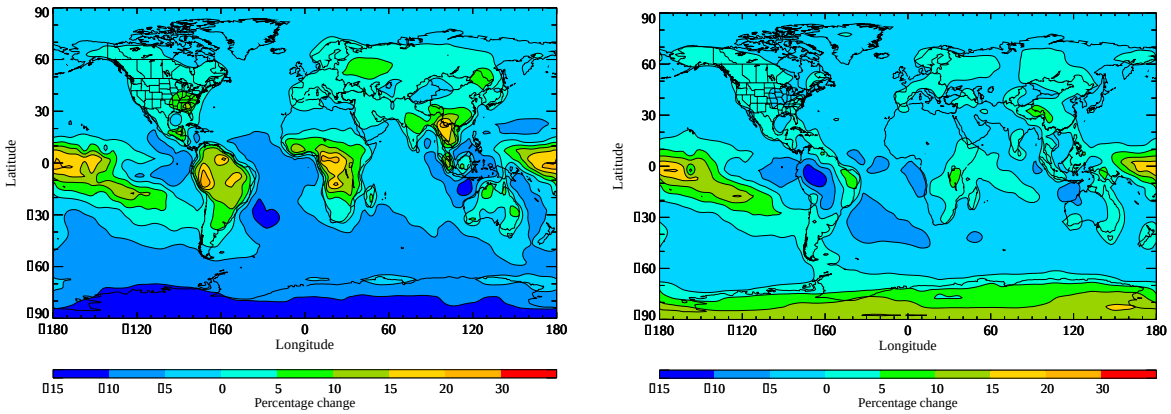


(e) (f)

**Fig. 2.** The percentage changes in (a) organic nitrates ($RONO_2$), (b) $NO_x$, (c) peroxy radicals ($RO_2$), (d) ozone ($O_3$), (e) nitrate radical ($NO_3$) (f) nitric acid ($HNO_3$) from base case to ISOP case. Note that percentage change= ((ISOP-base)*100)/base

The increased formation, transport and degradation of the isoprene-derived organic nitrates potentially has an impact on the global budget and distribution of $NO_x$, and thereby ozone. The recycling efficiency of $NO_x$ is reported to range from <5% to >50% for isoprene nitrates (Bates and Jacob, 2019; Horowitz et al., 2007; Paulot et al., 2009). In this study, the increased formation of isoprene derived organic nitrates in the ISOP simulation (Figure 2a) results in decreased $NO_x$ over the source regions (e.g. equatorial forested areas and the surrounding oceans) by up to 16% (Figure 2b). However, as a result of the decreased burden of isoprene derived peroxy radicals due to more rapid isomerization in the ISOP simulation, total $RO_2$ is decreased by up to 30% in the equatorial forested region (Figure 2c). Consequently, the formation of ozone is found to be reduced in the equatorial forested regions by up to 10% from the decreased $RO_2$ and $NO_x$ (Figure 2d).

The increased isoprene-related $HO_x$ recycling leads to increased $NO_x$ removal via reaction with OH in the ISOP simulation. This results in significant increased formation of $HNO_3$ (from the OH + $NO_2$ reaction) by 7 Tg/yr (3.3% from base case). The mixing ratios of $HNO_3$ have increased over the boreal and tropical regions (Figure 2f) and, along with the increased oxidising capacity, leading to an increase in the formation flux of $NO_3$ from the OH + $HNO_3$ reaction (2nd largest contributor of $NO_3$ formation with ~3% contribution) by 0.6 Tg/yr (7.1% from base case). The updated chemistry includes an additional $NO_3$ production pathway (~2% of the total $NO_3$ production) through the oxidation of MPAN (peroxymethacryloyl nitrate; OH initiated oxidation of the second-generation product from methyl vinyl ketone/methacrolein), which produced a significant amount (7.4 Tg/yr) of $NO_3$. The combination of OH + $HNO_3$ and OH + MPAN may result in an $NO_3$ concentration increase by up to 30% over tropical forested regions (Figure 2e). The increased $NO_3$ levels are therefore a consequence of the additional oxidising capacity associated with elevated $HO_x$

recycling and potentially further enhance the oxidizing capacity through initiating isoprene oxidation during night time (Brown et al., 2009).

The burden of formic acid (HCOOH) is found to decrease by 43.5% in the ISOP simulation (Table 1). This results partially from a decrease in the flux through the $O_3$ + isoprene reaction (because of the increased importance of OH-initiated removal), but also from significant updates to the product distribution assigned to that reaction. The yield of HCOOH from the reaction of isoprene with ozone is 17.5% in the updated mechanism, compared with 73% in the base case mechanism. The revised yield is compatible with about 30% formation of HCOOH from the reaction of the Criegee intermediate, $CH_2OO$, with $H_2O$ or $(H_2O)_2$; which is therefore intermediate to the yields of 54% and <10% reported by Nguyen et al. (2016) and Sheps et al. (2017), respectively, for the likely dominant $(H_2O)_2$ reaction. This update resulted in a decrease in the mixing ratios of HCOOH, with the greatest reductions of up to 80% experienced over the landmass in the tropics (Figure 3a) where both of the reactants, ozone and isoprene, are themselves also decreased. This result is therefore consistent with the results of Sheps et al. (2017) who used an overall yield of 6% for the formation of HCOOH from isoprene ozonolysis, followed by reaction of $CH_2OO$ with $(H_2O)_2$, and found a reduction of the global HCOOH levels by 10-90%. However, the reduction in HCOOH mixing ratios is in the opposite direction to that required by recent field measurements, that suggest the existence of large missing sources, which are currently unknown but could be a biogenic emission source from the oxidation of unspecified light-dependent biogenic VOCs (Millet et al., 2015; Bannan et al., 2017).

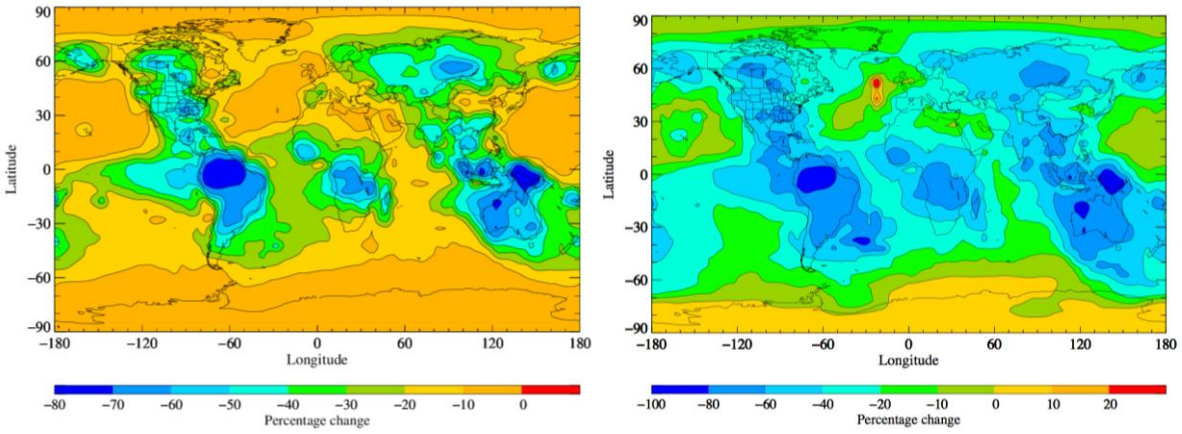


**Fig. 3.** The annual percentage change in (a) HCOOH mixing ratios between the base and ISOP (b) Criegee loss via reaction with HCOOH between the base and ISOP cases. Note that percentage change= ((ISOP-base)*100)/base

Previous studies show that the reaction of HCOOH with stabilised Criegee intermediates (sCIs) can be a dominant removal processes for tropospheric HCOOH (Chhantyal-Pun et al., 2018; Welz et al., 2014). The simulated decrease in tropospheric HCOOH due to incorporation of the new isoprene chemistry can overestimate the Criegee

intermediate concentrations due to the reduction of the Criegee loss by around 80% over the isoprene regions (Figure 3b). Given the importance of the linkage between HCOOH and Criegee fields, the burden to find HCOOH sources is increased.

## 4. Conclusions

Updated isoprene chemistry, based on the CRI v2.2 mechanism, has been implemented into the STOCHEM-CRI global 3D atmospheric chemistry and transport model. By doing so, an increase in $HO_x$ burden is found which results in a decrease in tropospheric isoprene mixing ratios in equatorial forested region, giving a slight improvement between model-measurement disagreements. However, reducing MEGAN isoprene emissions by a factor of 2 in the model brings the model isoprene levels into closer agreement with measured isoprene levels in Amazon, Surinam and Venezuela. Inclusion of the updated isoprene chemistry reduces the simulated atmospheric lifetime of $CH_4$ by 0.5 year. Through the additional chemistry implemented in ISOP, nitrate concentrations have been increasing by up to 30% in the areas with the highest vegetation levels, not only through an increase in $NO_3$ and $HNO_3$ mixing ratios but also an increase in alkyl nitrates especially isoprene-related nitrates. With regards to ozone mixing ratios, these were seen to decrease by up to 10% in the equatorial forested region. Formic acid is decreased over vegetated areas, which can decrease the loss rates of Criegee Intermediates in Amazon areas.

Satellite remote sensing of isoprene is now a reality, though current satellite technology limits its usefulness to high-emission regions (Fu et al., 2019). A thermal infrared sounder focused on optimized spectral resolution and range for remote sensing of isoprene along with PAN, ozone, and HCOOH, when combined with current remote sensing of ozone, $NO_2$ and HCHO in the ultraviolet region of the spectrum, would provide an ideal global dataset to test isoprene chemical mechanisms and better-constrain isoprene emissions and chemistry.

## Acknowledgement

DES and MAHK thank NERC (grant code-NE/K004905/1), Bristol ChemLabS and the Primary Science Teaching Trust under whose auspices various aspects of this work was supported. CJP and JLN work was carried out at Jet Propulsion Laboratory, California Institute of Technology, under contract with the National Aeronautics and Space Administration (NASA), and was supported by the Upper Atmosphere Research and Tropospheric Chemistry Programs. 

## References

Archibald, A.T., Cooke, M.C., Utembe, S.R., Shallcross, D.E., Derwent, R.G., Jenkin, M.E., 2010. Impacts of mechanistic changes on $HO_x$ formation and recycling in the oxidation of isoprene. Atmos. Chem. Phys. 10, 8097-8118.

Arnold, S.R., Spracklen, D.V., Williams, J., Yassaa, N., Sciare, J., Bonsang, B., Gros, V., Peeken, I., Lewis, A.C., Alvain, S., Moulin, C., 2009. Evaluation of the global oceanic

isoprene source and its impacts on marine organic carbon aerosol. Atmos. Chem. Phys. 9, 1253-1262.
Atkinson, R., Arey, J., 2003. Gas-phase tropospheric chemistry of biogenic volatile organic compounds. Atmos. Environ. 37, 197-219.
Bannan, T.J., Booth, A.M., Le Breton, M., Bacak, A., Muller, J.B.A., Leather, K.E., Khan, M.A.H., Lee, J.D., Dunmore, R.E., Hopkins, J.R., Fleming, Z.L., Sheps, L., Taatjes, C.A., Shallcross, D.E., Percival, C.J., 2017. Seasonality of formic acid (HCOOH) in London during the ClearfLo campaign. J. Geophys. Res. Atmos. 122, 12488-12498.
Barkley, M.P., Smedt, I.D., Roozendael, M.V., Kurosu, T.P., Chance, K., Arneth, A., Hagberg, D., Guenther, A., Paulot, F., Marais, E., Mao, J., 2013. Top-down isoprene emissions over tropical South America inferred from SCIAMACHY and OMI formaldehyde columns. J. Geophys. Res. Atmos. 118, 6849-6868.
Bates, K.H., Jacob, D.J., 2019. A new model mechanism for atmospheric oxidation of isoprene: global effects on oxidants, nitrogen oxides, organic products, and secondary organic aerosol. Atmos. Chem. Phys. 19, 9613-9640.
Bauwens, M., Stavrakou, T., Müller, J.–F., De Smedt, I., Roozendael, M.V., van der Werf, G.R., Wiedinmyer, C., Kaiser, J.W., Sindelarova, K., Guenther, A., 2016. Nine years of global hydrocarbon emissions based on source inversion of OMI formaldehyde observations. Atmos. Chem. Phys. 16, 10133-10158.
Borbon, A., Fontaine, H., Veillerot, M., Locoge, N., Galloo, J.C., Guillermo, R., 2001. An investigation into the traffic-related fraction of isoprene at an urban location. Atmos. Environ. 35, 3749-3760.
Brown, S.S., de Gouw, J.A., Warneke, C., Ryerson, T.B., Dubé, W.P., Atlas, E., Weber, R.J., Peltier, R.E., Neuman, J.A., Roberts, J.M., Swanson, A., Flocke, F., McKeen, S.A., Brioude, J., Sommariva, R., Trainer, M., Fehsenfeld, F.C., Ravishankara, A.R., 2009. Nocturnal isoprene oxidation over the Northeast United States in summer and its impact on reactive nitrogen partitioning and secondary organic aerosol. Atmos. Chem. Phys. 9, 3027-3042.
Caravan, R.L., Vansco, M.F., Au, K., Khan, M.A.H., Li, Y.–L., Winiberg, F.A.F., Zuraski, K., Lin, Y.–H., Chao, W., Trongsiriwat, N., Walsh, P.J., Osborn, D.L., Percival, C.J., Lin, J.–M. Jr, Shallcross, D.E., Sheps, L., Klippenstein, S.J., Taatjes, C.A., Lester, M.I., 2020. First direct kinetic measurements and theoretical predictions of an isoprene-derived Criegee intermediate with implications for aerosol formation. Proc. Nat. Acad. Sci. USA 117, 9733-9740.
Chen, X., Hulbert, D., Shepson, P.B., 1998. Measurement of the organic nitrate yield from OH reaction with isoprene. J. Geophys. Res. 103, 25563-25568.
Chhantyal-Pun, R., Khan, M.A.H., Martin, R., Zachhuber, N., Buras, Z.J., Percival, C.J., Shallcross, D.E., Orr-Ewing, A.J., 2019. Direct kinetic and atmospheric modelling studies of Criegee intermediate reactions with acetone. ACS Earth Space Chem. 3, 2363-2371.
Chhantyal-Pun, R., Rotavera, B., McGillen, M.R., Khan, M.A.H., Eskola, A.J., Caravan, R.L., Blacker, L., Tew, D.P., Osborn, D.L., Percival, C.J., Taatjes, C.A., Shallcross, D.E., Orr-Ewing, A.J., 2018. Criegee intermediate reactions with carboxylic acids: A potential source of secondary organic aerosol in the atmosphere. ACS Earth Space Chem. 2, 833-842.
Chuong, B., Stevens, P.S., 2002. Measurements of the kinetics of the OH-initiated oxidation of isoprene. J. Geophys. Res. 107, 4162.
Collins, W.J., Stevenson, D.S., Johnson, C.E., Derwent, R.G., 1999. Role of convection in determining the budget of odd hydrogen in the upper troposphere. J. Geophys. Res. 104, 26927.
Collins, W.J., Stevenson, D.S., Johnson, C.E., Derwent, R.G., 1997. Tropospheric ozone in a global-scale three-dimensional Lagrangian model and its response to $NO_x$ emission controls. J. Atmos. Chem. 26, 223-274.

Collins, W.J., Webber, C.P., Cox, P.M., Huntingford, C., Lowe, J., Sitch, S., Chadburn, S.E., Comyn-Platt, E., Harper, A.B., Hayman, G., Powell, T., 2018. Increased importance of methane reduction for a 1.5 degree target. Environ. Res. Lett. 13, 054003.
Cooke, M.C. Global modelling of atmospheric trace gases using the CRI mechanism. PhD Thesis, University of Bristol, UK, 2010.
Crutzen, P.J., Williams, J., Pöschl, U., Hoor, P., Fischer, H., Warneke, C., Holzinger, R., Hansel, A., Lindinger, W., Scheeren, B., Lelieveld, J., 2000. High spatial and temporal resolution measurements of primary organics and their oxidation products over the tropical forests of Surinam. Atmos. Environ. 34, 1161-1165.
Cullen, M.J., 1993. The unified forecast/climate model. Meteorol. Mag. 122, 81-94.
Delwiche, C., Sharkey, T., 1993. Rapid appearance of $^{13}C$ in biogenic isoprene when $^{13}CO_2$ is fed to intact leaves, Plant Cell Environ. 16, 587-591.
Derwent, R.G., Collins, W.J., Jenkin, M.E., Johnson, C.E., Stevenson, D.S., 2003. The global distribution of secondary particulate matter in a 3-D Lagrangian chemistry transport model. J. Atmos. Chem. 44, 57-95.
Donoso, L., Romero, R., Rondon, A., Fernandez, E., Oyola, P., Sanhueza, E., 1996. Natural and anthropogenic C2 to C6 hydrocarbons in the central-eastern Venezuelan atmosphere during the rainy season. J. Atmos. Chem. 25, 201-214.
Ehhalt, D.H., Rohrer, F., Wahner, A., 1992. Sources and distribution of $NO_x$ in the upper troposphere at northern mid-latitudes. J. Geophys. Res. 97, 3723-3738.
Emmerson, K.M., Galbally, I.E., Guenther, A.B., Paton-Walsh, C., Guerette, E.–A., Cope, M.E., Keywood, M.D., Lawson, S.J., Molloy, S.B., Dunne, E., Thatcher, M., Karl, T., Maleknia, S.D., 2016. Current estimates of biogenic emissions from eucalypts uncertain for southeast Australia. Atmos. Chem. Phys. 16, 6997-7011.
Fiore, A.M., Naik, V., Spracklen, D.V., Steiner, A., Unger, N., Prather, M., Bergmann, D., Cameron-Smith, P.J., Cionni, I., Collins, W.J., Dalsøren, S., Eyring, V., Folberth, G.A., Ginoux, P., Horowitz, L.W., Josse, B., Lamarque, J.–F., MacKenzie, I.A., Nagashima, T., O'Connor, F.M., Righi, M., Rumbold, S.T., Shindell, D.T., Skeie, R.B., Sudo, K., Szopa, S., Takemura, T., Zeng, G., 2012. Global air quality and climate. Chem. Soc. Rev. 41, 6663-6683.
Fisher, J.A., Jacob, D.J., Travis, K.R., Kim, P.S., Marais, E.A., Chan Miller, C., Yu, K., Zhu, L., Yantosca, R.M., Sulprizio, M.P., Mao, J., Wennberg, P.O., Crounse, J.D., Teng, A.P., Nguyen, T.B., St. Clair, J.M., Cohen, R.C., Romer, P., Nault, B.A., Wooldridge, P.J., Jimenez, J.L., Campuzano-Jost, P., Day, D.A., Hu, W., Shepson, P.B., Xiong, F., Blake, D.R., Golstein, A.H., Misztal, P.K., Hanisco, T.F., Wolfe, G.M., Ryerson, T.B., Wisthaler, A., Mikoviny, T., 2016. Organic nitrate chemistry and its implications for nitrogen budgets in an isoprene- and monoterpene-rich atmosphere: constraints from aircraft ($SEAC^4RS$) and ground-based (SOAS) observations in the Southeast US. Atmos. Chem. Phys. 16, 5969-5991.
Fu, D., Millet, D.B., Wells, K.C., Payne, V.H., Yu, S., Guenther, A., Eldering, A., 2019. Direct retrieval of isoprene from satellite-based infrared measurements. Nature Comm. 10, 3811.
Fuentes, J.D., Wang, D., Gu, L., 1999. Seasonal variations in isoprene emissions from a Boreal Aspen Forest. J. Appl. Meteorol. 38, 855-869.
Geng, F., Tie, X., Guenther, A., Li, G., Cao, J., Harley, P., 2011. Effect of isoprene emissions from major forests on ozone formation in the city of Shanghai, China. Atmos. Chem. Phys. 11, 10449-10459.
Greenberg, J.P., Zimmerman, P.R., 1984. Nonmethane hydrocarbons in remote tropical, continental and marine atmospheres. J. Geophys. Res. 89, 4767-4778.
Guenther, A.B., Jiang, X., Heald, C.L., Sakulyanontvittaya, T., Duhl, T., Emmons, L.K., Wang, X., 2012. The Model of Emissions of Gases and Aerosols from Nature version 2.1

(MEGAN2.1): An extended and updated framework for modeling biogenic emissions. Geosci. Model Dev. 5, 1471-1492.
Guenther, A., Hewitt, C.N., Erickson, D., Fall, R., Geron, C., Graedel, T., Harley, P., Klinger, L., Lerdau, M., McKay, W.A., Pierce, T., Scholes, B., Steinbrecher, R., Tallamraju, R., Taylor, J., Zimmerman, P., 1995. A global model of natural volatile organic emissions. J. Geophys. Res. 100, 8873-8892.
Helmig, D., Balsley, B., Davis, K., Kuck, L.R., Jensen, M., Bognar, J., Smith, T. Jr., Arrieta, R.V., Rodriguez, R., Birks, J.W., 1998. Vertical profiling and determination of landscape fluxes of biogenic non-methane hydrocarbons within the planetary boundary layer in the Peruvian Amazon. J. Geophys. Res. 103, 25519-25532.
Hewitt, C.N., Lee, J.D., MacKenzie, A.R., Barkley, M.P., Carslaw, N., Carver, G.D., Chappell, N.A., Coe, H., Collier, C., Commane, R., Davies, F., Davison, B., Di Carlo, P., Di Marco, C.F., Dorsey, J.R., Edwards, P.M., Evans, M.J., Fowler, D., Furneaux, K.L., Gallagher, M., Guenther, A., Heard, D.E., Helfter, C., Hopkins, J., Ingham, T., Irwin, M., Jones, C., Karunaharan, A., Langford, B., Lewis, A.C., Lim, S.F., MacDonald, S.M., Mahajan, A.S., Malpass, S., McFiggans, G., Mills, G., Misztal, P., Moller, S., Monks, P.S., Nemitz, E., Nicolas-Perea, V., Oetjen, H., Oram, D.E., Palmer, P.I., Phillips, G.J., Pike, R., Plane, J.M.C., Pugh, T., Pyle, J.A., Reeves, C.E., Robinson, N.H., Stewart, D., Stone, D., Whalley, L.K., Yin, X., 2010. Overview: oxidant and particle photochemical processes above a south-east Asian tropical rainforest (the OP3 project): introduction, rationale, location characteristics and tools. Atmos. Chem. Phys. 10, 169-199.
Holzinger, R., Sanhueza, E., Von Kuhlmann, R., Kleiss, B., Donoso, L., Crutzen, P.J., 2002. Diurnal cycles and seasonal variation of isoprene and its oxidation products in the tropical savanna atmosphere. Global Biogeochem. Cycles 16, 1074.
Horowitz, L.W., Fiore, A.M., Milly, G.P., Cohen, R.C., Perring, A., Wooldridge, P.J., Hess, P.G., Emmons, L.K., Lamarque, J.–F., 2007. Observational constraints on the chemistry of isoprene nitrates over the eastern United States. J. Geophys. Res. 112, D12S08.
Jenkin, M.E., Khan, M.A.H., Shallcross, D.E., Bergström, R., Simpson, D., Murphy, K.L.C., Rickard, A.R., 2019. The CRI v2.2 reduced degradation scheme for isoprene. Atmos. Environ. 212, 172-182.
Jenkin, M.E., Watson, L.A., Utembe, S.R., Shallcross, D.E., 2008. A Common Representative Intermediates (CRI) mechanism for VOC degradation. Part 1: Gas phase mechanism development. Atmos. Environ. 42, 7185-7195.
Jones, C.E., Hopkins, J.R., Lewis, A.C., 2011. In situ measurements of isoprene and monoterpenes within a south-east Asian tropical rainforest. Atmos. Chem. Phys. 11, 6971-6984.
Khan, M.A.H., Cooke, M.C., Utembe, S.R., Xiao, P., Derwent, R.G., Jenkin, M.E., Archibald, A.T., Maxwell, P., Morris, W.C., South, N., Percival, C.J., Shallcross, D.E., 2014. Reassessing the photochemical production of methanol from peroxy radical self and cross reactions using the STOCHEM-CRI global chemistry and transport model. Atmos. Environ. 99, 77-84.
Khan, M.A.H., Schlich, B.–L., Jenkin, M.E., Shallcross, B.M.A., Moseley, K, Walker, C., Morris, W.C., Derwent, R.G., Percival C.J., Shallcross, D.E., 2018. A two-decade anthropogenic and biogenic isoprene emissions study in a London urban background and a London urban traffic site. Atmosphere 9, 387.
Langford, B., Misztal, P.K., Nemitz, E., Davison, B., Helfter, C., Pugh, T.A.M., MacKenzie, A.R., Lim, S.F., Hewitt, C.N., 2010. Fluxes and concentrations of volatile organic compounds from a South-East Asian tropical rainforest. Atmos. Chem. Phys. 10, 8391-8412.

Lelieveld, J., Butler, T.M., Crowley, J.N., Dillon, T.J., Fischer, H., Ganzeveld, L., Harder, H., Lawrence, M.G., Martinez, M., Taraborrelli, D., Williams, J., 2008. Atmospheric oxidation capacity sustained by a tropical forest. Nature 452, 737-740.
Lin, Y.-H., Zhang, Z., Docherty, K.S., Zhang, H., Budisulistiorini, S.H., Rubitschun, C.L., Shaw, S.L., Knipping, E.M., Edgerton, E.S., Kleindienst, T.E., Gold, A., Surratt, J.D., 2012. Isoprene epoxydiols as precursors to secondary organic aerosol formation: Acid-catalyzed reactive uptake studies with authentic compounds. Environ. Sci. Technol. 46, 250-258.
Liu, Y., Brito, J., Dorris, M.R., Rivera-Rios, J.C., Seco, R., Bates, K.H., Artaxo, P., Duvoisin, S. Jr., Keutsch, F.N., Kim, S., Goldstein, A.H., Guenther, A.B., Manzi, A.O., Souza, R.A.F., Springston, S.R., Watson, T.B., McKinney, K.A., Martin, S.T., 2016. Isoprene photochemistry over the Amazon rainforest. Proc. Nat. Acad. Sci. USA 113, 6125-6130.
Lockwood, A.L., Shepson, P.B., Fiddler, M.N., Alaghmand, M., 2010. Isoprene nitrates: preparation, separation, identification, yields and atmospheric chemistry. Atmos. Chem. Phys. 10, 6169-6178.
Marais, E.A., Jacob, D.J., Guenther, A., Chance, K., Kurosu, T.P., Murphy, J.G., Reeves, C.E., Pye, H.O.T., 2014. Improved model of isoprene emissions in Africa using Ozone Monitoring Instrument (OMI) satellite observations of formaldehyde: implications for oxidants and particulate matter. Atmos. Chem. Phys. 14, 7693-7703.
Marais, E.A., Jacob, D.J., Kurosu, T.P., Chance, K., Murphy, J.G., Reeves, C., Mills, G., Casadio, S., Millet, D.B., Barkley, M.P., Paulot, F., Mao. J., 2012. Isoprene emissions in Africa inferred from OMI observations of formaldehyde columns. Atmos. Chem. Phys. 12, 6219-6235.
McFiggans, G., Mentel, T.F., Wildt, J., Pullinen, I., Kang, S., Kleist, E., Schmitt, S., Springer, M., Tillmann, R., Wu, C., Zhao, D., Hallquist, M., Faxon, C., Breton, M.L., Hallquist, A.M., Simpson, D., Bergström, R., Jenkin, M.E., Ehn, M., Thornton, J.A., Alfarra, M.R., Bannan, T.J., Percival, C.J., Priestley, M., Topping, D., Kiendler-Scharr, A., 2019. Secondary organic aerosol reduced by mixture of atmospheric vapours. Nature 565, 587-593.
Millet, D.B., Baasandorj, M., Farmer, D.K., Thornton, J.A., Baumann, K., Brophy, P., Chaliyakunnel, S., de Gouw, J.A., Graus, M., Hu, L., Koss, A., Lee, B.H., Lopez-Hilfiker, F.D., Neuman, J.A., Paulot, F., Pollack, I.B., Ryerson, T.B., Warneke, C., Williams, B.J., Xu, J., 2015. A large and ubiquitous source of atmospheric formic acid. Atmos. Chem. Phys. 15, 6283-6304.
Millet, D.B., Jacob, D.J., Boersma, K.F., Fu, T.–M., Kurosu, T.P., Chance, K., Heald, C.L., Guenther, A., 2008. Spatial distribution of isoprene emissions from North America derived from formaldehyde column measurements by the OMI satellite sensor. J. Geophys. Res. 113, D02307.
Mouchel-Vallon, C., Lee-Taylor, J., Hodzic, A., Artaxo, P., Aumont, B., Camredon, M., Gurarie, D., Jimenez, J.-L., Lenschow, D.H., Martin, S.T., Nascimento, J., Orlando, J.J., Palm, B.B., Shilling, J.E., Shrivastava, M., Madronich, S., 2020. Exploration of oxidative chemistry and secondary organic aerosol formation in the Amazon during the wet season: explicit modelling of the Manaus urban plume with GECKO-A. Atmos. Chem. Phys. 20, 5995-6014.
Müller, J.-F., Stavrakou, T., Peeters, J., 2019. Chemistry and deposition in the Model of Atmospheric composition at Global and Regional scales using Inversion Techniques for Trace gas Emissions (MAGRITTE v1.1)-Part 1: Chemical mechanism. Geosci. Model Dev. 12, 2307-2356.
Nguyen, T.B., Crounse, J.D., Schwantes, R.H., Teng, A.P., Bates, K.H., Zhang, X., Clair, J.M. St., Brune, W.H., Tyndall, G.S., Keutsch, F.N., Seinfeld, J.H., Wennberg, P.O., 2014. Overview of the Focused Isoprene eXperiment at the California Institute of Technology

(FIXCIT): mechanistic chamber studies on the oxidation of biogenic compounds. Atmos. Chem. Phys. 14, 13531-13549.
Nguyen, T.B., Tyndall, G.S., Crounse, J.D., Teng, A.P., Bates, K.H., Schwantes, R.H., Coggon, M.M., Zhang, L., Feiner, P., Miller, D.O., Skog, K.M., Rivera-Rios, J.C., Dorris, M., Olson, K.F., Koss, A., Wild, R.J., Brown, S.S., Goldstein, A.H., de Gouw, J.A., Brune, W.H., Keutsch, F.N., Seinfeld, J.H., Wennberg, P.O., 2016. Atmospheric fates of Criegee intermediates in the ozonolysis of isoprene. Phys. Chem. Chem. Phys. 18, 10241-10254.
Olivier, J.G., Bouwman, A.F., Berdowski, J.J., Veldt, C., Bloos, J.P., Visschedijk, A.J., Zandveld, P.Y., Haverlag, J.L., 1996. A set of global emission inventories of greenhouse gases and ozone-depleting substances for all anthropogenic and most natural sources on a per country basis and on 1 degree × 1 degree grid. Technical Report, Netherlands Environmental Assessment Agency.
Paulot, F., Crounse, J.D., Kjaergaard, H.G., Kroll, J.H., Seinfeld, J.H., Wennberg, P.O., 2009. Isoprene photooxidation: new insights into the production of acids and organic nitrates. Atmos. Chem. Phys. 9, 1479-1501.
Peeters, J., Nguyen, T.L., Vereecken, L., 2009. $HO_x$ radical generation in the oxidation of isoprene. Phys. Chem. Chem. Phys. 11, 5935-5939.
Peeters, J., Müller, J.–F., Stravrakou, T., Nguyen, V.S., 2014. Hydroxyl radical recycling in isoprene oxidation driven by hydrogen bonding and hydrogen tunneling: the upgraded LIM1 mechanism. J. Phys. Chem. A, 118, 8625-8643.
Percival, C.J., Welz, O., Eskola, A.J., Savee, J.D., Osborn, D.L., Topping, D.O., Lowe, D., Utembe, S.R., Bacak, A., McFiggans, G., Cooke, M.C., Xiao, P., Archibald, A.T., Jenkin, M.E., Derwent, R.G., Riipinen, I., Mok, D.W.K., Lee, E.P.F., Dyke, J.M., Taatjes, C.A., Shallcross, D.E., 2013. Regional and global impacts of Criegee intermediates on atmospheric sulfuric acid concentrations and first steps of aerosol formation. Faraday Discuss. 165, 45-73.
Prather, M.J., Holmes, C.D., Hsu, J., 2012. Reactive greenhouse gas scenarios: systematic exploration of uncertainties and the role of atmospheric chemistry. Geophys. Res. Lett., *39*, L09803.
Prinn, R.G., Huang, J., Weiss, R.F., Cunnold, D.M., Fraser, P.J., Simmonds, P.G., McCulloch, A., Harth, C., Reimann, S., Salameh, P., O'Doherty, S., Wang, R.H.J., Porter, L.W., Miller, B.R., Krummel, P.B., 2005. Evidence for variability of atmospheric hydroxyl radicals over the past quarter century. Geophys. Res. Lett. 32, L07809.
Pugh, T.A.M., Mackenzie, A.R., Hewitt, C.N., Langford, B., Edwards, P.M., Furneaux, K.L., Heard, D.E., Hopkins, J.R., Jones, C.E., Karunaharan, A., Lee, J., Mills, G., Misztal, P., Moller, S., Monks, P.S., Whalley, L.K., 2010. Simulating atmospheric composition over a South-East Asian tropical rainforest: performance of a chemistry box model. Atmos. Chem. Phys. 10, 279-298.
Rasmussen, R.A., Khalil, M.A., 1988. Isoprene over the Amazon basin. J. Geophys. Res. 93, 1417-1421.
Reimann, S., Pierluigi, C., Hofer, P., 2000. The anthropogenic fraction contribution to isoprene concentrations in a rural atmosphere. Atmos. Environ. 34, 109-115.
Romer, P.S., Duffey, K.C., Wooldridge, P.J., Allen, H.M., Ayres, B.R., Brown, S.S., Brune, W.H., Crounse, J.D., de Gouw, J., Draper, D.C., Feiner, P.A., Fry, J.L., Goldstein, A.H., Koss, A., Misztal, P.K., Nguyen, T.B., Olson, K., Teng, A.P., Wennberg, P.O., Wild, R.J., Zhang, L., Cohen, R.C., 2016. The lifetime of nitrogen oxides in an isoprene-dominated forest. Atmos. Chem. Phys. 16, 7623-7637.
Ryall, D.B., Maryon, R.H., Derwent, R.G., Simmonds, P.G., 1998. Modelling long-range transport of CFCs to Mace Head, Ireland. Quar. J. Royal Meteorol. Soc. 124, 417-446.

Schwantes, R.H., Teng, A.P., Nguyen, T.B., Coggon, M.M., Crounse, J.D., Clair, J.M. St., Zhang, X., Schilling, K.A., Seinfeld, J.H., Wennberg, P.O., 2015. Isoprene $NO_3$ oxidation products from the $RO_2$+$HO_2$ pathway. J. Phys. Chem. A 119, 10158-10171.
Seinfeld, J.H., Pandis, S.N. Atmospheric Chemistry and Physics, Wiley, 2006.
Sharkey, T.D., Yeh, S., 2001. Isoprene emission from plants. Ann. Rev. Plant Physiol. Plant Mol. Bio. 52, 407-436.
Sheps, L., Rotavera, B., Eskola, A.J., Osborn, D.L., Taatjes, C.A., Au, K., Shallcross, D.E., Khan, M.A.H., Percival, C.J., 2017. The reaction of Criegee intermediate $CH_2OO$ with water dimer: primary products and atmospheric impact. Phys. Chem. Chem. Phys. 19, 21970-21979.
Sindelarova, K., Granier, C., Bouarar, I., Guenther, A., Tilmes, S., Stavrakou, T., Müller, J.-F., Kuhn, U., Stefani, P., Knorr, W., 2014. Global data set of biogenic VOC emissions calculated by the MEGAN model over the last 30 years. Atmos. Chem. Phys. 14, 9317-9341.
Sonnemann, G.R.; Grygalashvyly, M., 2014. Global annual methane emission rate derived from its current atmospheric mixing ratio and estimated lifetime. Ann. Geophys. 32, 277-283.
Sprengnether, M., Demerjian, K.L., Donahue, N.M., Anderson, J.G., 2002. Product analysis of the OH oxidation of isoprene and 1,3-butadiene in the presence of NO. J. Geophys. Res. 107, 4269.
Stavrakou, T., Müller, J.–F., De Smedt, I., Van Roozendael, M., van der Werf, G.R., Giglio, L., Guenther, A., 2009. Global emissions of non-methane hydrocarbons deduced from SCIAMACHY formaldehyde columns through 2003-2006. Atmos. Chem. Phys. 9, 3663-3679.
Stevenson, D.S., Dentener, F.J., Schultz, M.G., Ellingsen, K., Van Noije, T.P., Wild, O., Zeng, G., Amann, M., Atherton, C.S., Bell, N., Bergmann, D.J., Bey, I., Butler, T., Cofala, J., Collins, W.J., Derwent, R.G., Dohert, R.M., Drevet, J., Eskes, H.J., Fiore, A.M., Gauss, M., Hauglustaine, D.A., Horowitz, L.W., Isaksen, I.S.A., Krol, M.C., Lamarque, J.-F., Lawrence, M.G., Montanaro, V., Müller, J.-F., Pitari, G., Prather, M.J., Pyle, J.A., Rast, S., Rodriguez, J.M., Sanderson, M.G., Savage, N.H., Shindell, D.T., Strahan, S.E., Sudo, K., Szopa, S., 2006. Multi-model ensemble simulations of present-day and ner-future tropospheric ozone. J. Geophys. Res., 111, D08301.
Utembe, S.R., Cooke, M.C., Archibald, A.T., Jenkin, M.E., Derwent, R.G., Shallcross, D.E., 2010. Using a reduced Common Representative Intermediates (CRI v2-R5) mechanism to simulate tropospheric ozone in a 3-D Lagrangian chemistry transport model. Atmos. Environ. 13, 1609-1622.
Watson, L.A., Shallcross, D.E., Utembe, S.R., Jenkin, M.E., 2008. A Common Representative Intermediates (CRI) mechanism for VOC degradation. Part 2: Gas phase mechanism reduction. Atmos. Environ. 42, 7196-7204.
Welz, O., Eskola, A.J., Sheps, L., Rotavera, B., Savee, J.D., Scheer, A.M., Osborn, D.L., Lowe, D., Booth, A.M., Xiao, P., Khan, M.A.H., Percival, C.J., Shallcross, D.E., Taatjes, C.A., 2014. Rate coefficients of C1 and C2 Criegee intermediate reactions with formic and acetic acid near the collision limit: Direct kinetics measurements and atmospheric implications. Angew. Chem. Int. Ed. 53, 4547-4550.
Wennberg, P.O., Bates, K.H., Crounse, J.D., Dodson, L.G., McVay, R.C., Mertens, L.A., Nguyen, T.B., Praske, E., Schwantes, R.H., Smarte, M.D., St Clair, J.M., Teng, A.P., Zhang, X., Seinfeld, J.H., 2018. Gas-phase reactions of isoprene and its major oxidation products. Chem. Rev. 118, 3337-3390.
Wolfe, G.M., Kaiser, J., Hanisco, T.F., Keutsch, F.N., de Gouw, J.A., Gilman, J.B., Graus, M., Hatch, C.D., Holloway, J., Horowitz, L.W., Lee, B.H., Lerner, B.M., Lopez-Hilifiker, F., Mao, J., Marvin, M.R., Peischl, J., Pollack, I.B., Roberts, J.M., Ryerson, T.B., Thornton, J.A.,

Veres, P.R., Warneke, C., 2016. Formaldehyde production from isoprene oxidation across $NO_x$ regimes. Atmos. Chem. Phys. 16, 2597-2610.
Xiong, F., McAvey, K.M., Pratt, K.A., Groff, C.J., Hostetler, M.A., Lipton, M.A., Starn, T.K., Seeley, J.V., Bertman, S.B., Teng, A.P., Crounse, J.D., Nguyen, T.B., Wennberg, P.O., Misztal, P.K., Goldstein, A.H., Guenther, A.B., Koss, A.R., Olson, K.F., de Gouw, J.A., Baumann, K., Edgerton, E.S., Feiner, P.A., Zhang, L., Miller, D.O., Brune, W.H., Shepson, P.B., 2015. Observation of isoprene hydroxynitrates in the southeastern United States and implications for the fate of $NO_x$. Atmos. Chem. Phys. 15, 11257-11272.
Zheng, Y., Unger, N., Tadić, J.M., Seco, R., Guenther, A.B., Barkley, M.P., Potosnak, M.J., Murray, L.T., Michalak, A.M., Qiu, X., Kim, S., Karl, T., Gu, L., Pallardy, S.G., 2017. Drought impacts on photosynthesis, isoprene emission and atmospheric formaldehyde in a mid-latitude forest. Atmos. Environ. 167, 190-201.
Zhu, J., Penner, J.E., Lin, G., Zhou, C., Xu, L., Zhuang, B., 2017. Mechanism of SOA formation determines magnitude of radiative effects. Proc. Nat. Acad. Sci. USA 114, 12685-12690.
Zimmerman, P.R., Greenberg, J.P., Westberg, C.E., 1988. Measurements of atmospheric hydrocarbons and biogenic emission fluxes in the Amazon boundary layer. J. Geophys. Res. 93, 1407-1416.